# Control-oriented closed-loop identification and input design in a wireless power transfer system

Shuaiqi Li, Qijun Deng[*], Zhifan Li and Wenshan Hu

*School of Electrical Engineering and Automation, Wuhan University, Wuhan 430072, China*
* Corresponding author, E-mail: dqj@whu.edu.cn

## Abstract

This study proposes a closed-loop identification scheme for a wireless power transfer (WPT) system that estimates the actual system model and uses it to design and update the controller. Due to factors such as coil misalignment, unknown loads, and capacitor aging, the initial controller may not be suitable for the actual WPT devices. Therefore, this paper focuses on estimating the model during closed-loop operation and updating the controller when performance requirements are not satisfied. To minimize disturbances to normal operation while achieving sufficient modeling accuracy for controller design, this study proposes a method for designing the input excitation signal to minimize output voltage fluctuations. Additionally, a robust controller design method based on the estimated model set is introduced to enhance closed-loop control performance. Experimental prototypes demonstrate the effectiveness of the identification and controller switching scheme.

## Introduction

Wireless power transfer (WPT) based on magnetic resonance coupling has garnered increasing attention due to its high efficiency and high-power transmission capabilities over moderate distances.[1]

Particularly in fields like electric vehicles, industrial robots, and underwater submersibles, WPT systems exhibit a series of advantages such as position free, minimal physical contact, high reliability, and no need for manual operation, thus being considered to have vast development potential[2–4]. However, most WPT system applications face a common challenge: variations in system parameters caused by factors such as coil misalignment, capacitor aging, and similar issues, which subsequently lead to changes in the closed-loop characteristics of the system. Thus, obtaining the current operating characteristics at low cost and designing an appropriate controller have become a new hotspot in WPT system control.

The initial controller (but unsatisfactory) design for WPT systems is generally based on theoretical models[5–7]. The manufacturing errors can cause discrepancies between the actual system and the theoretical model. Moreover, uncertainties in the receiving coil position and load impedance will introduce additional modeling errors into the system. The dynamic performance of the closed-loop system may change and even degrade when the parameters deviate from their initial values[7]. Therefore, accurate modeling before or during WPT operation is essential for designing a suitable controller.

Accurate WPT modeling using analytical methods is widely studied. A WPT system modeling method is proposed based on coupling mode theory[5], which describes voltage and current in both circuits using energy amplitude and phase. The method considers both amplitude and phase to obtain a time-invariant model. However, it does not account for control of the system under parameter uncertainty, and the nonlinear terms are complex to compute. A 9th-order linear model of the WPT system is derived using circuit analysis[6]. It employs dq decomposition to separate circuit parameters into DC and AC components, yielding a linear small-signal

model. However, this method is complex, requiring remodelling if parameters change and is valid only at specific operating points. A nonlinear WPT system is modeled using a generalized state-space averaging method[7], which approximates the system by focusing on low-order Fourier series terms for linearization. However, this method obtains a 17th-order model, complicating the controller design. In summary, analytical methods provide precise models but suffer from high computational complexity, making repetitive modeling difficult. Consequently, data-driven approaches are introduced in WPT to obtain sufficiently accurate models at a lower cost.

Data-driven modeling methods for WPT systems during operation have received significant attention in recent years. A system identification modeling method for WPT systems was introduced for the first time using the instrumental variable method[8], which derives models directly from data without measuring individual component parameters. However, it only applies to open-loop conditions and does not design a controller for closed-loop control. A simple scheme for WPT system identification is proposed[9], focusing on optimizing the input signal and improving modeling accuracy. However, it applies only to open-loop conditions and does not address WPT systems with changing parameters. A dynamic reduced-order modeling approach for WPT systems using an LPV Hammerstein model is proposed[10], accurately describing system output under variations in the inverter, rectifier bridge, load, and mutual inductance. However, it still optimizes the open-loop identification and does not consider the impact of the proposed methods on output control. Most WPT system identification studies focus on open-loop systems, while research on closed-loop systems, which are closer to real applications, remains limited.

In system identification, designing input signals to excite the main system modes for improved accuracy has always been a key research focus[9,11–14]. Such input signals are referred to as excitation signals. Input optimization was first introduced into identification for WPTs in 2023[9]. However it does not consider identification within a power-constrained closed-loop operating condition. To address this problem, the optimal input designs under various

constraints is proposed in[11–14]. These designs consider both distur-bance power and identification accuracy. However, practical imple-mentations on specific devices are rarely realized. In WPT systems, tolerance to fluctuations varies across different voltage levels, and the real-time calculation of optimal excitation signal for dynamic voltage changes remains unexplored. Compared with other exist-ing identification methods in WPT systems, modeling methods, the key contributions of this research can be summarized as:

(1) To model different WPT devices at low cost, a closed-loop online identification scheme is proposed.

(2) For minimal output voltage disturbance, an optimal excitation signal design with adaptive power is proposed.

(3) To maintain control performance under parameter distur-bance, an H∞ robust controller design method based on closed-loop identification is proposed.

## Preliminary

### System topology

As illustrated in Fig. 1, a WPT system with online identification consists of two main components: the power transmission module and the computing platform.

Where $V_d$ and $I_d$ are the inverter's DC voltage and current, $v_{C1}$ and $v_{C2}$ indicate the voltages across capacitors $C_1$ and $C_2$, $v_1$ and $i_1$ are the output voltage and current of the inverter, $v_2$, and $i_2$ is the input volt-age and current of the rectifier, $R_L$ is the load resistance, and $I_o$ is load current. $V_o$ is the load voltage denoted as $y$ in this paper, repre-senting the system output. Further, phase-shift control (PSC) is applied to the WPT system, so the input for the WPT system is the phase shift angle, denoted as $u$.

The power transmission module ensures the proper closed-loop operation of the WPT system, with voltage sampling data $y$ from the receiver sent wirelessly to the transmitter. The computing platform receives real-time input-output data to calculate new excitation signals and adjust controller parameters as needed.

### Modeling of the WPT system

The transfer function model of the WPT system is represented as $G_0 = Y(s)/U(s)$, where $Y(s)$ and $U(s)$ are Laplace transform of $\tilde{y}(t)$ and $\tilde{u}(t)$, respectively. Here, $\tilde{y}(t)$ and $\tilde{u}(t)$ denote the small signal compo-nents of $y(t)$ and $u(t)$, correspondingly. The initial component param-eters are listed in Table 1. For the parameters given in Table 1, the small-signal model of the WPT system can be derived using the D-Q decomposition method[6], resulting in a 9th-order transfer function representation:

**Table 1.** System design parameters.

| Parameters | Values |
| --- | --- |
| Switching frequency $f_0$ | 92 kHz |
| DC voltage $V_D$ | 50 V |
| Self-inductance of primary coil $L_1$ | 117 μH |
| Self-inductance of secondary coil $L_2$ | 116 μH |
| Primary resonant capacitance $C_1$ | 26 nF |
| Secondary resonant capacitance $C_2$ | 25.4 nF |
| Mutual inductance $M$ | 37 μH |
| Filter capacitance $C_f$ | 450 μF |
| Load resistance $R_L$ | 35 Ω |
| Sampling time $T_s$ | 1 ms |

$$G_0(s) = \frac{\begin{aligned}-2.9e7s^7 + 2.4e14s^6 - 5.1e19s^5 + 5.3e25s^4 - ...\\ ... - 7.2e31s^3 - 1.3e38s^2 - 1.5e43s - 1.0e48\end{aligned}}{\begin{aligned}s^9 + 2.8e05s^8 + 2.8e12s^7 + 5.8e17s^6 + 1.9e24s^5 + ...\\ ... + 2.7e29s^4 + 3.9e34s^3 + 2.2e39s^2 + 1.5e44s + 4.4e46\end{aligned}} \tag{1}$$

### Parameter perturbations analysis

During the operation, the WPT system model changes randomly due to factors such as coil movement and gradual variations in load. Setting the parameters listed in Table 1 as the initial parameters, the bode plots of $G_0$ under varying condition of $M$ is shown in Fig. 2.

As shown in Fig. 2a, when the mutual inductance gradually increases, the dominant pole shifts to the right, but it remains in the negative half-plane. Meanwhile, other poles gradually move to the left. In Fig. 2b, it can be seen that regardless of the variation in the load resistance, there is only one dominant pole. In fact, under reso-nant conditions, the system's main characteristics are represented by the final filter circuit. Under typical conditions with a mutual inductance of 35 μH, the system has only one dominant pole, which can be described by a low-order model. This conclusion still holds when the mutual inductance is no less than 15 μH. If the mutual inductance is too small, the model order needs to be increased, but this can be achieved by adjusting the identification algorithm parameters, without incurring additional costs. Therefore, for ease of analysis, this paper uses a first-order system to characterize the system's main dynamic characteristics.

The variation of the dominant pole of $G_0$ affects the dynamic performance of the closed-loop system $[G_0 C]$, potentially leading to degraded control performance or instability. Therefore, this paper employs a system identification method to online estimate the system model at the start of charging and update the controller to ensure the control performance.
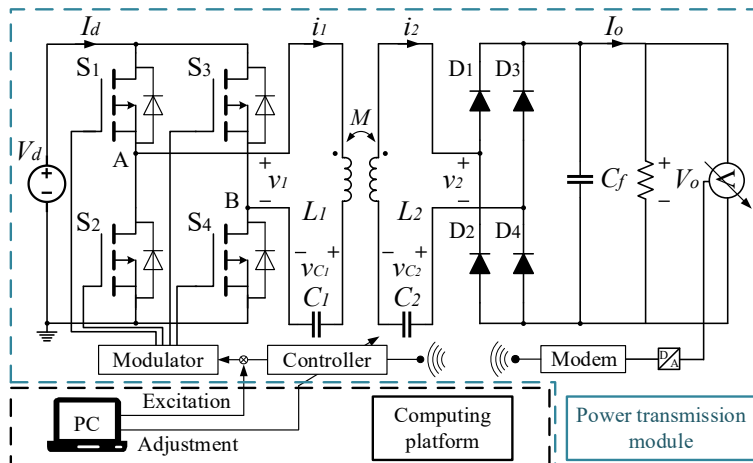


**Fig. 1** The topology of the WPT system.
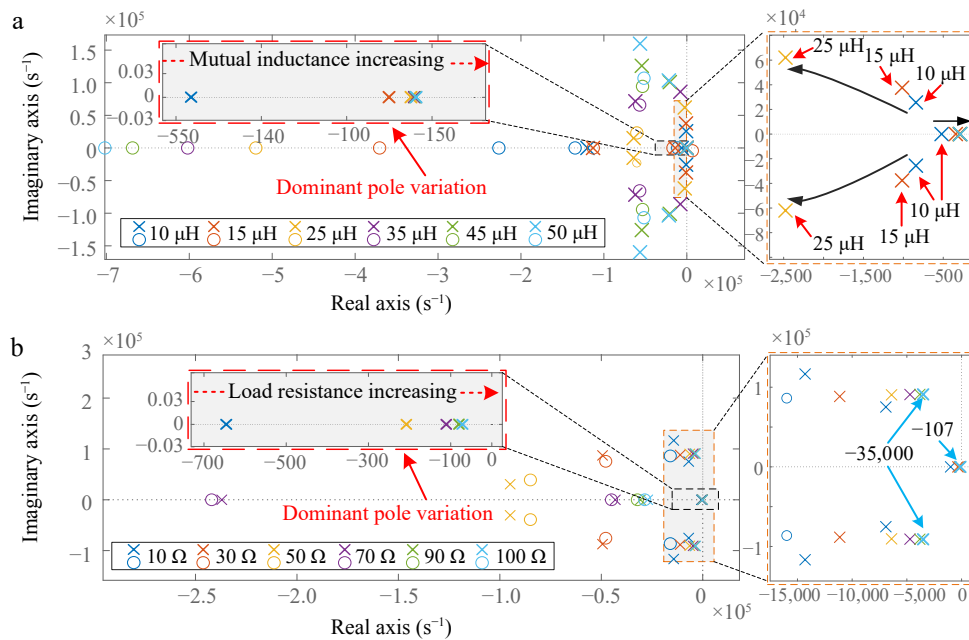
**Fig. 2** Zero-pole distribution plot. (a) Zero-pole distribution under mutual inductance. (b) Zero-pole distribution under load resistance variation.

## Proposed identification and control scheme

### Identification experimental design

The identification scheme of the closed-loop WPT system $[G_0\ C_i]$ are given in Fig. 3. $V_{ref}$ is the voltage reference value. $u$ and $y$ indicate the input and output signals of $G_0$, respectively. $v$ represents measurement noise. The unknown WPT system $G_0$ is controlled by an initial controller $C_i$, its control performance is not fully satisfactory and thus requires replacement with a new controller. To design an improved H∞ robust controller, it is necessary to obtain an estimated model $\hat{G}$ of the real system $G_0$ within the operating closed-loop system $[G_0\ C]$. This allows for defining a parametric uncertainty region $\mathcal{D}$ centered around $\hat{G}$ and containing the $G_0$ with some chosen probability $\beta$. To accurately identify the model, it is necessary to apply excitation signal $R$ to the system, which causes disturbances during operation. The purpose of the WPT closed-loop identification experiment is to obtain a sufficiently accurate model and a small uncertainty region $\mathcal{D}$ with minimal output power disturbances. The model parameter of $G_0$ and $\hat{G}$ is represented as $\theta^*$ and $\hat{\theta}$, respectively. The size of the estimated $\mathcal{D}$ is a function of the covariance matrix $P_\theta$ of $\hat{\theta}$. Consequently, it also depends on the power spectrum $\Phi_r(\omega)$ of $R$ used for identification.

The system input-output behavior is described by $G_0$, and represented as output-error model form[8]:

$$\begin{cases} x(k) = G(s,\theta)u(k) = \dfrac{B(z^{-1},\theta)}{A(z^{-1},\theta)}u(k) \\ y(k) = x(k) + v(k) \end{cases} \quad (2)$$

where, $z^{-1}$ is the differentiation operator, and $v(k)$ assumed to be zero-mean white noise with finite variance. Polynomials $A(z^{-1})$ and $B(z^{-1})$ take the forms:
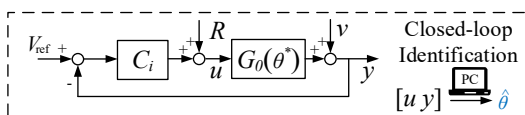
$$\begin{aligned} A(s,\theta) &= z^{-n_a} + a_1 z^{-n_a+1} + \cdots + a_{n_a} \\ B(s,\theta) &= b_0 z^{-n_b} + \cdots + b_{n_b} \\ n_b &\leqslant n_a \end{aligned} \quad (3)$$

The model can be reformulated as a linear system of equations:

$$z(k) = h^T(k)\theta + v(k) \quad (4)$$

where, superscript $T$ denotes the vector/matrix transpose, $h^T(k) = [-y(k-1), \ldots, -y(k-n_a), u(k-1), \ldots, u(k-n_b)]$ is the data vector, model parameter $\theta = [a_1, a_2, \ldots, a_{n_a}, b_1, b_2, \ldots, b_{nb}]$ is the parameter vector. It's worth noting that Eqn (4) is now linear in $\theta$, which allows the Parameter Estimation Method (PEM) to estimate $\theta$. To obtain the estimated value $\hat{\theta}$, this paper employs the recursive least squares algorithm with a forgetting factor[15–17], which is a type of PEM aimed at minimizing the prediction error:

$$\lim_{N\to\infty}\frac{1}{N}\sum_{k=1}^{N}E\left(y(k) - G\left(z^{-1},\hat{\theta}\right)u(k)\right) \quad (5)$$

Based on the statistical characteristics of $\hat{\theta}$ analyzed in Bombois et al. [13], an uncertainty region $\mathcal{D}$ can be defined around the determined model, which encompasses the unknown actual system $G_0$ at any desired probability level $\chi$:

$$\mathcal{D}\left(\hat{\theta}_N, P_\theta\right) = \left\{G(z^{-1},\theta)\,\middle|\,\theta \in U, U = \left\{\theta\,\middle|\,\left(\theta - \hat{\theta}_N\right)^{\mathrm{T}}P_\theta^{-1}\left(\theta - \hat{\theta}_N\right) < \chi\right\}\right\} \quad (6)$$

The size of the uncertainty region $\mathcal{D}$ is a function of $P_\theta$ and $\Phi_r(\omega)$[13].

The application of external signal $R$ to the loop during the identification introduces disturbances on the normal operation signals[13]. These disturbances can lead to a loss of system stability and potentially damage to the unknown loads. Thus, this study explores an LMI-based (Linear Matrix Inequality) optimal design of $\Phi_r(\omega)$ to achieve the optimal excitation signal $R$ under constraints of disturbance power and accuracy. To incorporate $\Phi_r(\omega)$ into the design process of the LMI optimization problem, it is necessary to first linearize it. For finite-dimensional spectral parameterization, such as the form shown in Eqn (7), we choose $e^{-jwk}$ as the basis function. At this point, the input spectrum $\Phi_u(\omega)$ can be expressed as the form of a finite impulse response (FIR) filter, thereby introducing the finite-dimensional constraints from the FIR filter design. Any spectrum can



**Fig. 3** Identification scheme diagram.

be expanded with FIR representation to a certain degree of accuracy, a method that is generally applicable. The spectrum for the input excitation sequence $R$ is defined as[12]:

$$\Phi_r\left(e^{j\omega}\right) = \frac{1}{2}c_0 + \sum_{k=1}^{M_c-1} c_k e^{-j\omega k} \qquad (7)$$

where, $c_0, c_1, \ldots, c_{Mc-1}$ are the parameters to be optimized and $M_c$ is the selected FIR filter order. The optimal excitation signal $R$ is obtained by shaping white noise through a $M_c$ order FIR filter. For a given excitation signal length $N$, the optimal power spectrum $\Phi_r(\omega)$ can be determined by minimizing the following cost function $\mathcal{J}_r$, thereby minimizing the output disturbance power[12].

$$\mathcal{J}_r = \frac{1}{2\pi}\int_{-\pi}^{\pi} \pi\left(\left|G_0\left(e^{j\omega}\right)S_i\left(e^{j\omega}\right)\right|^2\right)\Phi_r(\omega)d\omega \qquad (8)$$

where, $S_i = 1/(1 + C_i G_0)$. In the practical application of WPT systems, tolerable voltage fluctuations vary with different $V_{ref}$, and the signal-to-noise ratio of the A/D sampler also differs in different measurement ranges. Thus, dynamic adjustment of adaptive output power bound $y_{ub}^{pow}$ and $y_{lb}^{pow}$ of $y$ is necessary based on $V_{ref}$ and noise of $y$, i.e. $y_{ub}^{pow} = (k_a V_{ref} - \Phi_v)/|G_0(j\omega)|^2$, where $k_a$ is the adaptive coefficient and $\Phi_v$ is the estimated power of $v$. $y_{lb}^{pow}$ is typically set to a small value greater than 0. The optimal solution of $\Phi_r(\omega)$ for a reduced-order WPT model is then obtained by solving the LMI optimization problem described as follows:

$$\underset{\Phi_u}{\text{minimize}} \ \alpha$$

$$\text{subject to} \ \left|T(\omega)\frac{G_0(\omega,\theta_0) - G(\omega,\theta)}{G(\omega,\theta)}\right|^2 \leqslant \gamma^2, \forall\omega$$

$$(\theta - \theta_0)^T P^{-1}(\Phi_u)(\theta - \theta_0) \leqslant \chi, \qquad (9)$$

$$y_{lb}^{pow} \leqslant \frac{1}{2\pi}\int_{-\pi}^{\pi}\Phi_y(\omega)d\omega \leqslant y_{ub}^{pow},$$

$$\Phi_u(\omega) \geqslant 0, \forall\omega$$

Under resonant conditions, the system model order can be significantly reduced and approximated as a first-order model[9]. In this case, $\chi$ is a chi-squared distribution with 2 degrees of freedom and a 0.95 confidence level, i.e. $\chi^{(20.95)} = 5.99$. The solution to this LMI optimization problem is obtained using the MATLAB 'MOOSE2' toolbox[18].

### Design of the H∞ robust controller

As described in Eqn (6), $G_0$ is probabilistically contained within $\mathcal{D}$. Therefore, the requirement for the new controller is to ensure that the closed-loop system of the actual system $G_0$ achieves adequate H∞ performance under the modeling errors represented by all models in $\mathcal{D}$. PEM provides an estimated plant model and a confidence ellipsoid for the identified parameters in Eqn (5). In closed-loop identification, $\mathcal{D}$ is obtained that contains the actual system with a certain probability $\beta$, and which is defined as a set of parametrized transfer functions:

$$\mathcal{D} = \left\{G(z,\theta) \mid G(z,\theta) = \frac{A(\theta)}{B(\theta)} \text{, and } \theta \in \mathbf{U}\right\} \qquad (10)$$

The system input-output behavior is described by $G_0$, and represented as output-error model form[8]. In this paper, the differences between the region $\mathcal{D}$ models are considered as modeling uncertainties and are introduced into the H∞ robust control scheme. The actual system model exists in the region $\mathcal{D}$ with probability level $\chi$, which can be described by multiplicative modeling uncertainty. Consequently, the controller design for the system $G_0$, considering the region $\mathcal{D}$, can be reformulated as a standard H∞ optimal control problem, leveraging small gain theory, as shown in Fig. 4.

In Fig. 4, $P$ represents a generalized plant with uncertainty, $d$ is the external disturbance, $G_n$ is the nominal model, and $C$ is the H∞

controller. Weighting functions $W_u$ and $W_p$ reflect system performance, while $W_t$ captures frequency-domain parameter uncertainty. $W_u$ and $W_p$ are easily designed[7,19], and $W_t$ accounts for modeling errors across all relevant frequencies. [$z_p$, $z_u$, $z_t$] represents the constructed system output evaluation function used to assess the impact of disturbances. $W_t$ is calculated as follows:

$$|W_t(j\omega)| \geqslant |\Delta W_t(j\omega)| \geqslant \left|\frac{G_s(j\omega) - G_n(j\omega)}{G_n(j\omega)}\right|, \quad G_s(j\omega) \in \mathcal{D} \qquad (11)$$

where, $G_s$ represents all the independently identified models within the confidence ellipse (described by Eqn 6), and $G_n$ is selected as the center of the ellipse. In this paper, $G_n = -16.59/(1-0.75z^{-1})$, which is obtained through experimentation. A simplified method is proposed to construct $W_t$, representing the worst-case parameter deviations in $\mathcal{D}$, as shown in Fig. 5.

Plot the magnitude error between the $G_n$ and all models in region $\mathcal{D}$, with the maximum error designated as $W_t$ (red line in Fig. 5). Then, $W_t$ is obtained using a linear fitting method implemented in the MATLAB mathematical toolbox as[20]:

$$W_t = \frac{-4.539z + 10.57}{z^2 - 2.371z + 1.597} \qquad (12)$$

Based on the weighting functions www and the identified nominal model $G(\hat{\theta})$, the reduced-order controller $C$ can be obtained using the robust control toolbox in MATLAB：

$$C = \frac{-0.001302z + 0.001094}{z^2 - 1.761z + 0.7613} \qquad (13)$$

## Experimental verification

The experimental prototype, shown in Fig. 6, consists of a full-bridge inverter, powered by a DC source (REG75030). The transmission coils are made of 9 turns of 3,000 × 0.01 mm Litz wire. The Schottky diode is used in the AC/DC rectifier to produce a DC voltage output, which is measured with an oscilloscope (Tektronix MSO2024B). An ARM (STM32F407VGT) and an FPGA (XC6SLX9-3TOG1441) are utilized for generating control signals, collecting input/output data, and communicating with the PC.

### Identification experiments

The WPT system starts with the initial controller at the start of transmission. Input-output data is collected to estimate the initial model. The optimal input spectrum $\Phi_r(\omega)$ is then designed based on this initial model using Eqns (7)–(9). By setting $M_c = 10$, the optimal
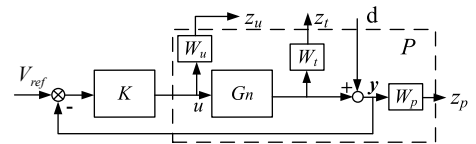
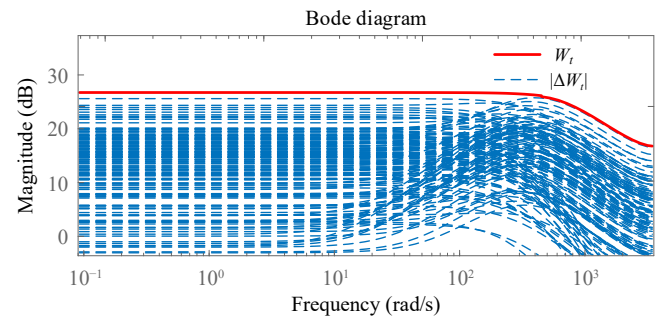**Fig. 4** Structure diagram of H∞ problem for the WPT system.

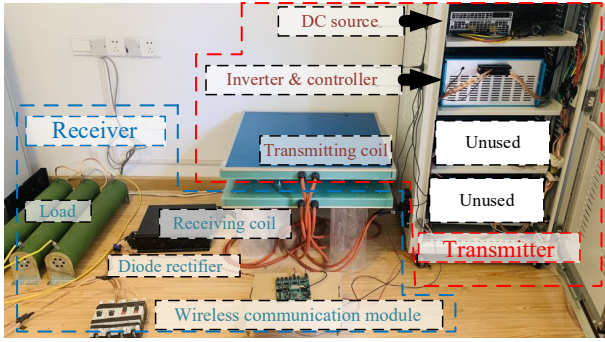**Fig. 5** Structure diagram of H∞ problem for the WPT system.

**Fig. 6** Circuit topology for the WPT system under consideration.

spectrum in the form of a FIR filter is obtained as:

$$H(z) = 0.2863 + 0.3119z^{-1} + 0.3311z^{-2} + 0.344z^{-3} + 0.3505z^{-4} + ...$$
$$...0.3505z^{-5} + 0.344z^{-6} + 0.3311z^{-7} + 0.3118z^{-8} + 0.2862z^{-9} \quad (14)$$

The Bode plot of $H$ is provided in Fig. 7. It can be observed that the excitation signal for the current WPT system requires higher gain at mid-to-low frequencies. The discrete sequence $R_k = [r_1, r_2, ..., r_N]$ of the excitation signal $R$ in the $k$-th experiment can be obtained by filtering a white noise signal with a variance of 0.1 through the FIR filter, as shown in Eqn (14).

Figure 2 indicates that, in the resonant state, the WPT system possesses only one pole. Consequently, a first-order system is sufficient to describe the system's dynamic performance[9].
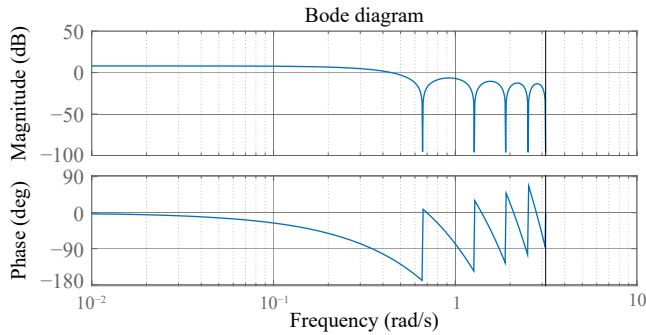


**Fig. 7** Bode plot of the optimal spectrum $H$.
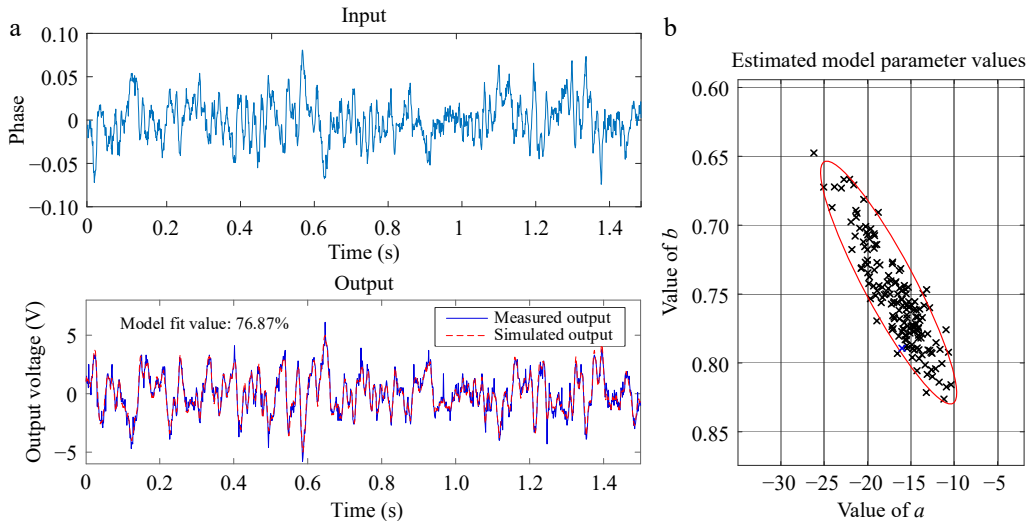
$$G_0 = \frac{a}{1 - bz^{-1}} \quad (15)$$

The identification results from the closed-loop data is presented in Fig. 8a. Due to sampling errors, experimental duration, and limitations in excitation power, the fit value based on the optimal input is 76.87%, which is adequate for controller design. Figure 8b shows the identification confidence ellipses for the controller design, corresponding to the case shown in Fig. 5.

To validate the superiority of the proposed method, comparisons are made with two typical identification signals (i.e. white noise and PRBS signal), and the resulting fit values are presented in Table 2.

For a sequence of sampled voltage disturbances, $\tilde{y}(t) = y(t) - Y$, where the disturbance is obtained by subtracting the equilibrium point $Y$ from the actual value $y(t)$, its power can be calculated using the following formula:

$$P = \frac{1}{N} \sum_{n=0}^{N-1} |y[n]|^2 \quad (16)$$

where, $N$ is the length of the signal, and $y[n]$ is the sampled value of the discrete signal. By calculating this, we ensure a fair comparison of different excitation signals under the same output disturbance power. It can be observered that under the same output disturbance power, the proposed method achieves significantly higher fit value.

## Control experiments

This study employs closed-loop identification to obtain the actual WPT model and design an appropriate controller, addressing the performance limitations of the initial controller. As illustrated in Fig. 9, the initial controller exhibits a 10% overshoot in voltage during transitions from 30 to 40 V and from 40 to 50 V, with a settling time of approximately 100 ms. When control performance at point A in Fig. 9a fails to meet the specified requirements, system excitation and identification are initiated at point B. Following the identification of the system model and the subsequent controller design, a controller switch occurs at point C. Ultimately, point D in Fig. 9c demonstrates the improved control performance of the

**Table 2.** Comparison of various typical signals.

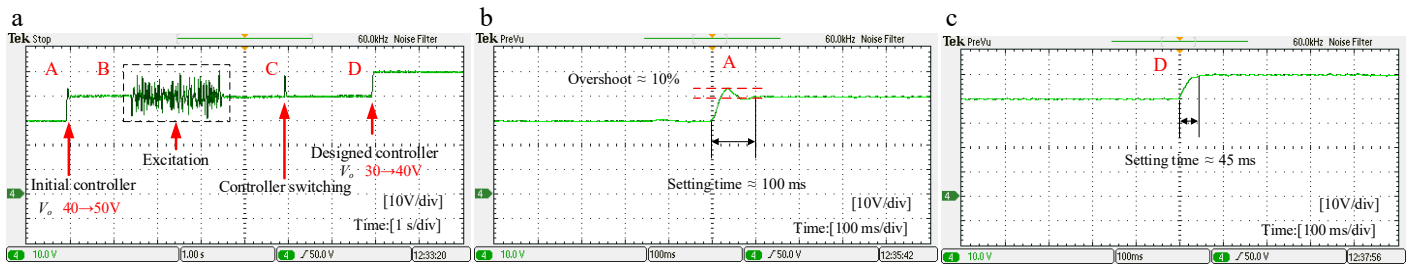|  | Proposed method | White noise | PRBS |
|---|---|---|---|
| Output power (w) | 0.40 | 0.40 | 0.41 |
| Fit value (%) | 76.87 | 55.19 | 68.04 |



**Fig. 8** Identification results. (a) Portion of input and output generated from the LMI optimization excitation signal. (b) The estimated model parameter values.

**Fig. 9** Voltage variation control experiment based on system identification. (a) Overall view of voltage step response, system excitation, and controller switching. (b) $V_0$ increase from 30 to 40 V. (c) $V_0$ increase from 40 to 50 V.
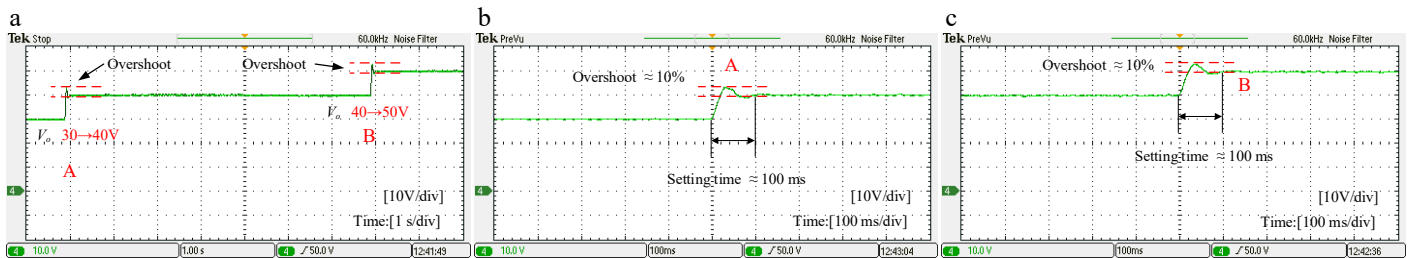


**Fig. 10** Voltage variation control experiment with constant controller. (a) Overall view of voltage step response. (b) $V_0$ increase from 30 to 40 V. (c) $V_o$ increase from 40 to 50 V.

updated closed-loop system, indicating a significant enhancement in system performance post-controller update. It can be observed that the output disturbance generated by the excitation signal is still relatively large. However, it can be observed that the disturbance generated by the excitation signal is still relatively large. To further reduce the input disturbance, this can be achieved by either lowering the value of $y_{ub}^{\mathrm{pow}}$ in the LMI optimization Eqn (9) or by limiting the amplitude of the input excitation signal shown in Fig. 9a. For comparison, Fig. 10 illustrates that for the same WPT system, the output voltage transitions from 30 to 40 V and from 40 to 50 V exhibit similar closed-loop performance without switching controllers. This further confirms the effectiveness of the proposed closed-loop identification framework.

## Conclusions

In this article, a closed-loop identification and controller design approach has been proposed for WPT systems. Due to the variability of the parameters, it is impossible to design a controller that fits all WPT devices. Therefore, to minimize the disturbance to the normal operation of the WPT system, this study proposes a closed-loop identification scheme with minimal disturbance. This method helps obtain a usable model with minimal output disturbance power and design a controller that can be updated in real-time. The proposed optimal excitation signal is compared with common white noise and PRBS sequences, and experimental results indicate that, under consistent output disturbance power, the optimal signal designed in this paper has a higher fit value. Additionally, controller switching experiments also demonstrate the effectiveness of the closed-loop identification scheme.

## Author contributions

The roles and contributions to the paper of each author are described as follows: study conception and design: Deng Q; data collection: Li S, Li Z; analysis and interpretation of results: Li S; draft manuscript preparation: Li S, Li Z; manuscript review and editing: Li Z, Hu W. All authors have read and agreed to the published version of the manuscript.

## Data availability

All data included in this study are available upon request from the corresponding author.

## Acknowledgments

## Conflict of interest

The authors declare that they have no conflict of interest. Qijun Deng is the Editorial Board member of *Wireless Power Transfer* who was blinded from reviewing or making decisions on the manuscript. The article was subject to the journal's standard procedures, with peer-review handled independently of this Editorial Board member and the research groups.

## Dates

## References

1. Hui SYR, Zhong W, Lee CK. 2014. A critical review of recent progress in mid-range wireless power transfer. *IEEE Transactions on Power Electronics* 29(9):4500−11

2. Sekiya H, Tokano K, Zhu W, Komiyama Y, Nguyen K. 2023. Design procedure of load-independent class-E WPT systems and its application in robot arm. *IEEE Transactions on Industrial Electronics* 70(10):10014−23

3. Li S, Mi CC. 2015. Wireless power transfer for electric vehicle applications. *IEEE Journal of Emerging and Selected Topics in Power Electronics* 3(1):4−17

4. Si P, Hu AP, Malpas S, Budgett D. 2008. A frequency control method for regulating wireless power to implantable devices. *IEEE Transactions on Biomedical Circuits and Systems* 2(1):22−29

5. Chen C, Zhou H, Deng Q, Hu W, Yu Y, et al. 2018. Modeling and decoupled control of inductive power transfer to implement constant

current/voltage charging and ZVS operating for electric vehicles. *IEEE Access* 6:59917−28

6. Deng Q, Wang Z, Chen C, Czarkowski D, Kazimierczuk M. K, et al. 2019. Modeling and control of inductive power transfer system supplied by multiphase phase-controlled inverter. *IEEE Transactions on Power Electronics* 34(9):9303−15

7. Liang Y, Sun P, Wu X, Zhou H, Sun J, et al. 2022. H∞ robust control for ICPT system with selected weighting function considering parameter perturbations. *IEEE Transactions on Power Electronics* 37(11):13914−29

8. Chen F, Garnier H, Deng Q, Kazimierczuk MK, Zhuan X. 2020. Control-oriented modeling of wireless power transfer systems with phase-shift control. *IEEE Transactions on Power Electronics* 35(2):2119−34

9. Li Z, Deng Q, Chen F, Sun P, Liu J, et al. 2023. Receding horizon D-optimal input design for identification of wireless power transfer systems. *IEEE Journal of Emerging and Selected Topics in Power Electronics* 11(3):3597−606

10. Chen F, Hu H, Zhao L, Padilla A, Hou J. 2023. A linear parameter-varying Hammerstein model for dynamic modeling of WPT systems. *IEEE Transactions on Power Electronics* 38(12):16230−44

11. Hjalmarsson H. 2005. From experiment design to closed-loop control. *Automatica* 41(3):393−438

12. Jansson H, Hjalmarsson H. 2005. Input design via LMIs admitting frequency-wise model specifications in confidence regions. *IEEE Transactions on Automatic Control* 50(10):1534−49

13. Bombois X, Scorletti G, Gevers M, Van den Hof PMJ, Hildebrand R. 2006. Least costly identification experiment for control. *Automatica* 42(10):1651−62

14. Jakowluk W, Świercz M. 2023. Application-oriented input spectrum design in closed-loop identification. *Applied Sciences* 13(11):6552

15. Isermann R, Münchhof M. 2011. *Identification of dynamic systems: an introduction with applications*. Vol. 85. Berlin, Heidelberg: Springer. doi: 10.1007/978-3-540-78879-9

16. Paleologu C, Benesty J, Ciochina S. 2008. A robust variable forgetting factor recursive least-squares algorithm for system identification. *IEEE Signal Processing Letters* 15:597−600

17. Young PC. 2011. *Recursive estimation and time-series analysis: an introduction for the student and practitioner*. Berlin, Heidelberg: Springer Science & Business Media. doi: 10.1007/978-3-642-21981-8

18. Annergren M, Larsson CA, Hjalmarsson H, Bombois X, Wahlberg B. 2017. Application-oriented input design in system identification: Optimal input design for control [applications of control]. *IEEE Control Systems Magazine* 37(2):31−56

19. Gu DW, Petkov PH, Konstantinov MM. 2005. *Robust Control Design with MATLAB®*. London, UK: Springer. doi: 10.1007/b135806

20. Liang Y, Sun P, Wu X, He L, Sun J, et al. 2024. Improved *H∞* control for input-series–output-series multichannel inductive power transfer system considering parameter inconsistency and load perturbation. *IEEE Transactions on Power Electronics* 39(5):6477−91